The Potential of MEMS for Advancing Experiments and Modeling in Cell Mechanics

O. Loh · A. Vaziri · H.D. Espinosa

Abstract Response to mechanical stimuli largely dictates cellular form and function. A host of extraordinary yet unexplained responses have been identified within the hierarchical cell structure. As experimental and model-based investigations in cell mechanics advance, the underlying structure-function mechanisms dictating these responses emerge. Here we explore the potential of microelectromechanical systems (MEMS) for advancing understanding of cell mechanics. To motivate the discussion, existing experimental techniques are summarized. Interrelated model-based approaches, which aim to interpret or predict observed results, are also outlined. We then focus on a representative set of MEMS-based devices designed for investigations in cell mechanics and point to the fact that, while these devices have yet to maximize their functionality through higher levels of sensor/actuator integration, they are highly complementary to existing techniques. In closing, novel MEMS sensor and actuator schemes that have yet to materialize in this field are discussed to motivate the next generation of MEMS for investigations in cell mechanics.

Keywords Cell mechanics · Cell adhesion · Biomechanics · MEMS · Modeling

Introduction

Healthy cells exist in a state of homeostasis in which they transduce mechanical forces to biochemical signals and vice versa. Much of the cell form and function are influenced through these transduction pathways. Numerous experimental and model-based approaches investigate the role of mechanics in dictating cellular response, mechanisms of cell adhesion, and the mechanics of biomolecules [1]. Relevant mechanics span multiple orders of magnitude in spatial and temporal dimensions. On short time scales, mechanical stimulation of a cell surface receptor can trigger immediate reorganization of molecular assemblies within the nucleus and cytoplasm [2]. Contractile bundles form or dissociate in response to biochemical and physical stimuli [3]. A striking example of slower response lies in human mesenchymal stem cells. Simply by altering the stiffness of their substrate, these cells are differentially directed along neuronal, muscle, or bone lineages [4]. Here the cell must sense the stiffness of its surroundings, likely by contracting to balance internal tension with traction forces [5, 6]. These forces must then be distributed within the cell and trigger biochemical signals which in turn induce a biological response (see [7] for review of mechanotransduction pathways and signaling).

Alterations to the mechanics of a cell and subcellular components may lead to loss of functionality. Red blood cells, which are naturally biconcave, undergo large elastic deformation to squeeze through tiny capillaries. However, malaria-infected red blood cells experience structural changes as the disease progresses, eventually becoming spherical with shear modulus increasing by an order of magnitude [8]. Ultimately, this stiffening and morphological change prevents the red blood cells from passing through capillaries, resulting in blockage and eventual organ failure [9].

While these and numerous other phenomena involving the mechanics of cells have been identified, the underlying mechanisms remain largely unknown. Difficulties explaining these observations are compounded by the hierarchical nature of cells, with relevant processes spanning multiple orders of magnitude in spatial and temporal dimensions. Local events (e.g., junction formation in cell adhesion) tend to be locally mediated and progress rapidly. Global responses

O. Loh · H.D. Espinosa (✉, SEM member)
Mechanical Engineering, Northwestern University,
2145 Sheridan Rd,
Evanston, IL 60208-3111, USA
e-mail: espinosa@northwestern.edu

A. Vaziri
Division of Engineering and Applied Sciences, Harvard University,
29 Oxford St, Pierce 316,
Cambridge, MA 02138, USA

generally require changes in gene expression and take place over longer time periods [10]. Consequently, it is difficult to use a single experimental technique or model to capture both the locally-mediated processes that may eventually lead to a global response and the global response itself.

Driven by applications to biotechnology, physiology, and medicine, as well as interests of basic research, a significant body of literature describes novel devices and models designed to build understanding of observed phenomena in cells, including transduction, adhesion, motility, and proliferation. Here we explore the potential of microelectromechanical systems (MEMS) to further advance the field. For comparison, common (non-MEMS-based) experimental techniques are first summarized. While representative references are given, these techniques have been thoroughly reviewed elsewhere (see for example [11, 12]). To further motivate the discussion, methods of modeling cellular mechanics and their complementary relationship to experimental cell mechanics are reviewed. A representative set of existing micromechanical and microelectromechanical systems are discussed and compared with other techniques. Finally, the potential of alternative MEMS sensors and actuators to benefit the study of cell mechanics is discussed to motivate the next generation of MEMS.

Motivation for Use of MEMS

Within the hierarchical structure of cells, the mechanisms dictating cellular response to mechanical stimuli span several orders of magnitude in spatial and temporal dimensions. Accordingly, relevant forces and displacements are widespread. To provide context, Table 1 summarizes representative orders of magnitude of relevant cellular parameters (also

see Hochmuth [13] for an illustrative table of "natural" SI units in cellular processes). As experimental techniques improve, we gain the ability to probe the mechanics of subcellular systems at different scales, which in turn dictate the cellular response. Advances in molecular and continuum modeling complement experimental progress by helping to explain the mechanisms underlying experimentally-observed phenomena.

Common Experimental Techniques

To motivate our discussion of MEMS for cell mechanics investigations, some commonly-used (non-MEMS-based) experimental techniques are summarized for later comparison. Figure 1 depicts these techniques schematically. As shown in Fig. 2, the functional ranges of these techniques span many orders of magnitude. For further details and references on these techniques, the reader is referred to other reviews (see for example [11, 12]). Techniques are grouped according to their interaction with the cell: active techniques that impose a time-varying mechanical stimulus to elicit a response, and; passive techniques designed to observe cellular response to a constant condition.

Active techniques

Micropipette aspiration is perhaps the most widely-used technique in experimental cell mechanics. The cell is aspirated into a glass pipette with an inner diameter smaller than the cell, causing it to deform [14]. The extent to which the cell enters the pipette is quantified by optical microscope and used to infer mechanical properties of the cell. Fine force resolutions are possible as loading is controlled by the applied pressure (with typical resolutions of 0.1 Pa

Table 1 Summary of order of magnitude of parameters commonly measured in cell mechanics

Parameter	Characteristic	Order	Ref.
Force [N]	RNA extension	10^{-12}	[157]
	N- or E-cadherin/cadherin bond rupture	10^{-11}	[20]
	P-selectin/ligand bond rupture	10^{-10}	[158]
	Chicken embryo fibroblast traction	10^{-8}	[127]
	Rabbit patellar tendon fibroblast tensile failure	10^{-6}	[159]
	Heart cell contraction	10^{-5}	[129]
Length [m]	DsDNA, dsRNA persistence length	10^{-8}	[157]
	HIV diameter, RNA length	10^{-7}	[160]
	Human heart myocyte contraction	10^{-7}	[161]
	Human red blood cell diameter	10^{-5}	[11]
	Human DNA	1	[162]
Elastic modulus [Pa]	Human mesenchymal stem cells	10^{2}	[163]
	Human umbilical vein endothelial cells	10^{3}	[23]
	DNA	10^{8}	[164]
	Collagen fibril	10^{8}	[133]

Fig. 1 Schematic depiction of common experimental techniques employed in cell mechanics
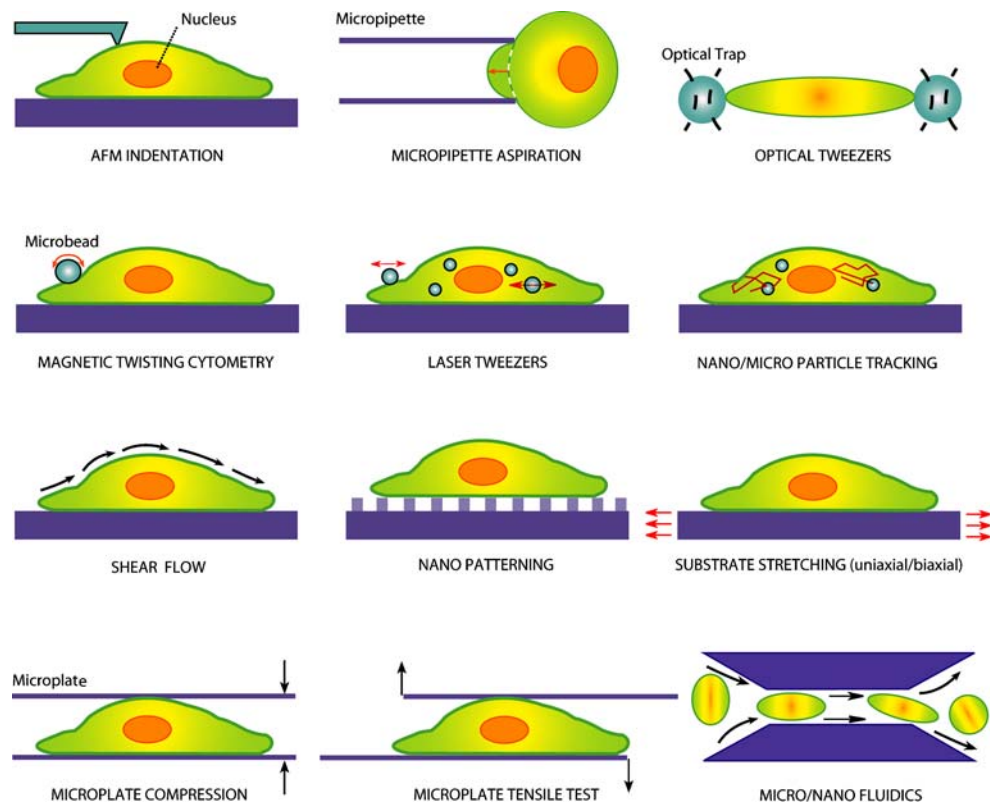
([13]) and the inner diameter of the pipette. However, this technique often requires the cell to endure large deformations, making it incompatible with some cell types. Furthermore, the geometry of the cell-pipette interface creates a complex state of stress, requiring indirect determination of properties. Examples of studies conducted by micropipette aspiration include investigation of the flow of blood cells through small vessels and the influence of chemical and mechanical stimuli on cell behavior [13].

Atomic force microscopy (AFM) has been used to probe levels of cellular mechanics ranging from global viscoelasticity [15] and elastic properties [16, 17] down to properties of isolated cell nuclei [18] and the strength of individual cadherin-cadherin bonds [19–22]. Here the probe is often functionalized to promote a specific type of binding. AFM can be combined with various forms of optical microscopy, for example fluorescence or total internal reflectance fluorescence microscopy [23], for simultaneous imaging of the cell.

The displacement and force resolution of commercially-available atomic force microscopes enable this broad range of studies. However, the ultra-sensitivity of the AFM, which is achieved using the reflection of a laser beam from a flexible cantilever, imposes intrinsic constraints. For example, the possible range of forces measured by a single probe depends in part on the cantilever stiffness as the photodiodes used to detect probe deflection are designed to measure only small displacements. Thus, the stiffness of the probe is

chosen to produce measurable deflections in response to force ranges of interest and no single probe may be used to investigate the full range of phenomena listed above. This constraint is common to many experimental techniques. The experimental setup for AFM-based studies can also be complex. Operation in aqueous environments, often required to maintain normal cell function, may be complicated by fluid-probe interaction and reflection or refraction of the laser used for sensing. Further difficulties arise for non-adherent cells [12].

Optical or laser traps (or tweezers) are used to manipulate functionalized beads tethered to the structure of interest [8, 24–33]. The laser refracts as it passes through a bead. By conservation of momentum, the changing photon momentum results in a change of the bead's momentum and thus a force on the bead toward the focal point of the laser (the point of greatest intensity) [31]. This force is proportional to the perpendicular distance from the optic axis of the trap. Resulting bead displacements may be measured by tracking the refracted beam with photodiodes, or by analysis of optical images of the interference patterns or the beads themselves. At the finest scales, optical traps have been used in numerous single-molecule studies [32], for example to study the kinetics of RNA unfolding [33]. On larger scales, this technique has been used to study global cell properties, such as changes in stiffness of red blood cells with the progression of malaria by manipulating beads adhered to malaria-infected red blood cells [8]. While this

Fig. 2 Comparison of reported functional ranges of techniques for studying cellular mechanics. Note that the ranges reported here are not necessarily attainable with a single device. For example, the finest resolution and maximum force for AFM are not achieved simultaneously using a single cantilever. Note, all values reported in this table are meant only to demonstrate order of magnitude with no greater precision. References for these values are listed in Table 2
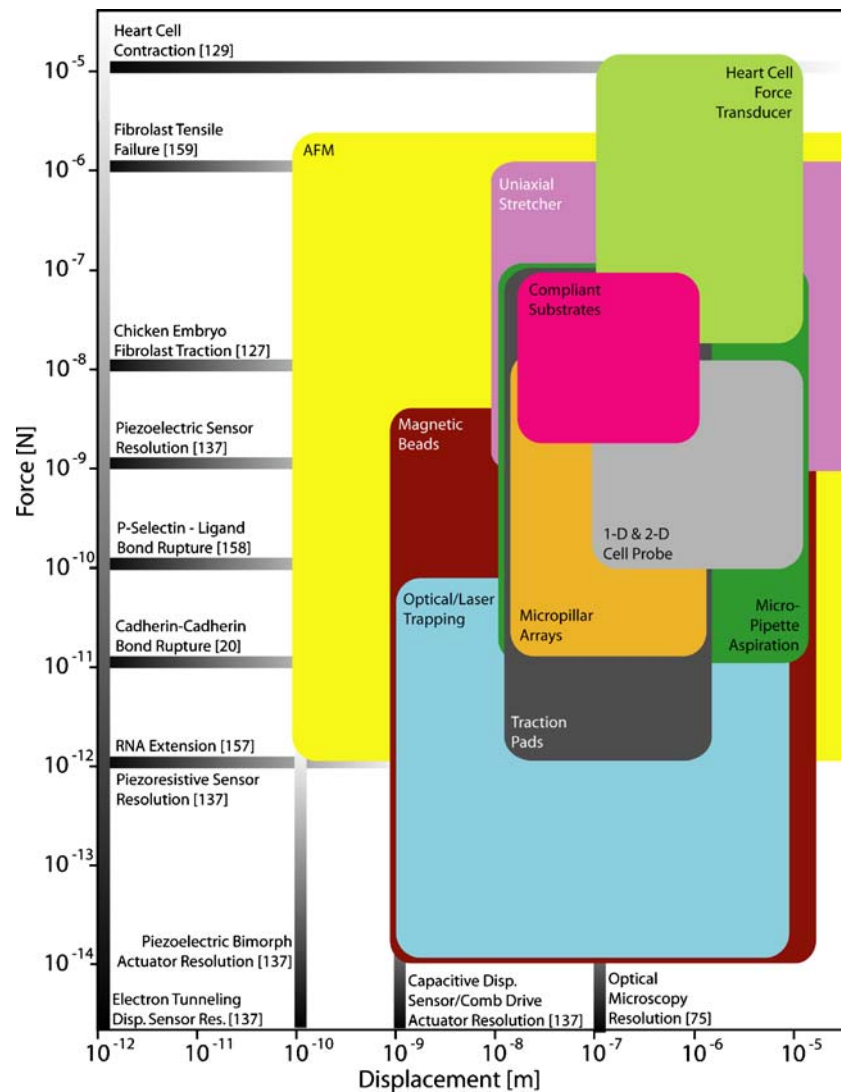
technique affords the finest force resolution (see Fig. 2), it is generally limited to experiments requiring forces below 0.1 nN. At the risk of damaging the specimen, higher power lasers may be used to stiffen the optical trap and apply greater forces.

Similar to optical traps, magnetic beads may be manipulated by an externally-generated magnetic field to apply loading [34–39]. This method has been used for example to quantify mechanical or transport properties of motor proteins, DNA, and on a larger scale, entire cells [35]. Using magnetic tweezers to load *E. coli* DNA, it was shown that small variations in applied force or torque switch the DNA gyrase between three modes of activity [40]. In this experiment, the magnetic bead was tethered to the substrate by a single DNA molecule. By translating or rotating the external magnetic field, variable forces or torques were applied to the DNA. Magnetic beads have the added advantage that torques can be applied to the beads simply by rotating the external field. While torque generation is possible with

optical traps (see for example [41]), it requires a modified experimental setup. The unfavorable scaling of magnetic forces at small scales (magnetic forces scale at best with the square of their characteristic dimension [42]) is often a limiting factor in these systems, often requiring relatively large beads in comparison to the sample size.

There are several variations to the magnetic tweezers. Magnetic twisting cytometry [38, 39, 43] utilizes magnetic beads with aligned fields. The beads' fields may be aligned by applying a weak magnetic field as they settle on the cell, or by magnetizing them after adhering to the cell. The magnetically-aligned beads are then twisted by a strong external magnetic field with which the beads attempt to align. The degree to which the beads rotate (as measured from the changing magnetic signal) under the applied torque provides information, for example, regarding force transmission between the cell membrane and cytoskeleton [38]. In magnetic bead microrheometry, strong magnetic pulses are used to apply localized loading [34]. The resulting

deformation of the cell is imaged by tracking non-magnetic beads dispersed on the surface of the cell. One drawback to magnetic methods is the large beads that are often required to achieve adequate forces [44]. These are made necessary by the fact that magnetic forces do not scale favorably with decreasing size. Furthermore, as with optical traps, the specific versus non-specific interactions between the cell membrane and beads are not well-characterized [44].

Flow-induced shear is commonly used to load adherent cells within a flow chamber. A major advantage to fluid flow methods is the fact that they naturally create a more cell-friendly environment than some other techniques. Dong and Lei [45] used this technique to study rolling adhesion of white blood cells in shear flow. The flow chamber was designed to allow measurement of cell rolling velocity, deformation, and the cell-substrate contact length from optical images. By altering cell deformability through treatment with cytochalasin B, the authors showed for example that increasing cell compliance decreases rolling velocity. This was attributed to the reduced flow disturbance and increased contact area that result from flow-induced deformation [45]. Another example of the use of flow-induced shear is in investigating the influence of laminar shear stress on cell proliferation [46]. Bovine aortic endothelial cells exposed to steady flow showed a reduction in the rate of cell proliferation. Proliferation was completely arrested at high shear stresses [46].

Cells adhered to flexible substrates may be strained by stretching or bending the substrate. Variations of this technique allow for uniaxial or biaxial loading. These may be used for example to reproduce forces in bone tissue (for a summary, see [47]). In another example, a device was made to study the mechanical properties and effects of stretch on human alveolar epithelial cells (lung cells) [48, 49]. Here the substrate, which was supported on a ring-shaped holder, was stretched by applying vacuum beneath the perimeter (outside the ring holder) [48]. Magnetic twisting cytometry (see above) was then used to measure the local properties of the stretched cells. By tracking the beads, local strains were also determined. These experiments demonstrated that cell viscoelasticity increases with stretching and that chemical disruption of the actin cytoskeleton inhibits this response, suggesting the important role of the actin cytoskeleton in the cells' mechanical response [48]. The importance of cell-cell junctions was also demonstrated with the same apparatus by showing the ability of confluent cells to withstand greater tension when exposed to thrombin than subconfluent cells [49].

Passive techniques

Multiple-particle-tracking microrheology is a passive technique in which micro or nanoparticles are dispersed on the cell membrane or injected into the cytoplasm of a cell and then tracked to map local displacements or mechanical properties of the cell [44, 50, 51]. Motion is mapped by tracking the path of the particles over time through successive digital images [50]. Properties of the surrounding material may be inferred by observing the Brownian motion of the particles within the cytoplasm (see following section for a quantitative analysis of Brownian motion). This has been used for example to assess heterogeneity in the mechanical properties of the cytoplasm [44, 51]. Laser tracking microrheology is an alternative method for measuring embedded bead displacements [52]. Here a low-powered laser is focused on a bead embedded in the filamentous network. The bead causes far-field scatter of the beam. The resulting deflection from the optic axis is observed by a four-quadrant detector, much like in an AFM, providing sub-nanometer and near-microsecond spatial and temporal resolutions.

Multiple techniques infer the direction and/or magnitude of cellular traction forces by imaging deformation of a compliant substrate. Some use extremely thin, soft membranes which wrinkle in response to traction forces generated by an adhering cell [53, 54]. While the wrinkles are readily observed, there is no direct way to translate the complex wrinkle patterns into quantifiable forces. Related techniques use particles embedded in a flexible substrate as fiduciaries to map in-plane deformation of the substrate [55–58]. These maps are formed by tracking the position of the particles through successive digital images. For substrates of known stiffness, these displacements can be transformed into traction vectors. However, quantification of forces from measured deformations of a continuous substrate is computationally taxing due to complex strain distributions. Imaging resolution and the accuracy of the substrate stiffness calibration, combined with the force computation method, dictate the overall resolution of the technique. A variation of this technique, using closely-spaced compliant microfabricated pillars that bend in response to traction forces [59–63], will be discussed later in conjunction with other microfabricated devices.

Substrates are selectively patterned with biofunctionalized regions to observe effects on cellular response. Substrates patterned by microcontact printing [64] have been used for example to demonstrate the ability to switch endothelial cells between growth, differentiation, or apoptosis by controlling the geometry of their spreading [65]. Other studies investigate the effects of adhesive ligand spacing on cell motility and focal adhesion dynamics [66].

The techniques summarized here, both active and passive, have facilitated great advances in the understanding of cell mechanics. However, some common limitations need to be overcome. Many of the techniques described above require indirect methods of computing properties such as elastic modulus or viscoelasticity. This is in part due to complex

constraint and loading conditions. These conditions also complicate comparisons with models of cell mechanics. While high force and displacement resolutions are reported, the figures do not always consider uncertainties in assumptions made in the indirect calculation of material properties. Finally, these techniques are typically limited to a single type of stimulus or measurement as the generally complex and bulky exterior equipment required for these studies limits the number of simultaneous interactions with the cell. For example, simultaneously probing a cell with multiple AFMs would be impractical. At the same time, it may be desirable to probe multiple points on the cell, both to stimulate response and sense changes in mechanical properties.

Fundamental limits to resolution

Noise imposes fundamental limits on the displacement and force resolution of the techniques described herein. Mechanical-thermal noise caused by Brownian motion creates uncertainty in probe position and effectively creates a minimum functional limit, below which forces and displacements cannot be applied or measured. Noise in associated sensing components, such as that in electronic components, further limits the resolution of these devices. Interestingly, this noise can be described in the same general terms for nearly any system. Gabrielson [67] shows that the mechanical-thermal noise of even the most complex systems can be described in terms of the dissipative elements in the system. Assuming thermal equilibrium, the energy gained from thermal vibrations is balanced by that dissipated through damping [68]. Thus the noise sources can be modeled with the simple addition of a force generator at each damper in the characteristic mass-spring-damper representation.

Johnson–Nyquist noise [69, 70], originally used to describe thermal agitation of electrons within an electrical conductor, may be generalized to describe mechanical-thermal vibrations in micromechanical experiments. These vibrations tend to dominate noise in micromechanical experiments (e.g. trapped beads or compliant probes). For example, thermal vibrations in AFM probes create uncertainty in the probe position and thus the measured force. As shown in Fig. 2, AFM force measurements (at room temperature) are limited to approximately 0.1 pN resolution, whereas sub-attonewton force detection has been demonstrated using silicon cantilevers at millikelvin temperatures [71]. When in static contact, the mean-square displacement of the cantilever tip caused by Brownian motion may be defined as [72]:

$$\langle z_{th}^2 \rangle = \frac{4k_B T B}{K \omega_0 Q},$$

where k_B is Boltzmann's constant, T is the temperature, B is the bandwidth, and K and ω_0 are the stiffness and resonance frequency of the cantilever respectively. The resulting thermal noise equivalent force then is $F = K\sqrt{\langle z_{th}^2 \rangle}$ [72]. Note that this is analogous to the Johnson–Nyquist noise-generated voltage across a resistor in an electrical system.

The displacement-sensing system (e.g. the optical-electrical system of an AFM) is another source of noise. Assuming a noise density n_{ds} in the displacement-sensing system, an additional term $(n_{ds}^2 B)$ is added to the total noise displacement. From this, the minimum detectable force in static contact AFM as defined by the Brownian motion and sensor noise is computed assuming a linear spring, namely [72]:

$$F_{min} = K\sqrt{\langle z_{th}^2 \rangle + n_{ds}^2 B}.$$

Noise limits in other techniques are described similarly. Gittes and Schmidt [73] present a generalized description of mechanical-thermal noise for microscopic probe systems in terms of the viscous drag. This approach is particularly relevant to cell mechanics where experiments typically take place at low Reynolds numbers, making inertial forces insignificant compared to the viscous drag [73]. For a "position-clamp" experiment where the probe is held stationary by feedback to observe time-varying forces, the uncertainty in the force is formulated in terms of the hydrodynamic drag coefficient γ of the probe (e.g. bead or AFM probe) [73]:

$$\Delta F_{rms} = \sqrt{4\gamma k_B T f_s},$$

where f_s is the cutoff frequency, above which the signal is filtered by a low-pass filter. Here Gittes and Schmidt point out a common misconception. Increasing the probe stiffness does not necessarily decrease force uncertainty as it does not depend directly on probe stiffness (unless electronic noise dominates, in which case the decreased stiffness will allow larger displacements to overcome the noise) [73]. Instead the resolution is improved by reducing the drag or, at the expense of temporal resolution, by reducing the cutoff frequency [73].

The relatively small drag coefficient of optical and magnetic beads is in part responsible for their finer force and displacement resolutions as compared to that of the AFM [73]. At the present, AFM cantilevers cannot be made significantly smaller as they rely on the reflection of a laser beam for displacement detection. Making them smaller would create diffraction and reduce the signal intensity. This suggests an advantage to using self-sensing MEMS devices. By eliminating external sensing schemes, the probes can be made smaller to reduce drag.

Noise in MEMS, which are the focus of this review, is described in similar terms. In this case, Johnson–Nyquist noise (in the electrical-thermal domain) and flicker noise (or $1/f$ noise) are more directly coupled to the system. As an example, we take the noise effective force as presented by Villanueva et al. [74] for a piezoresistive (self-sensing)

cantilever used for detection of intermolecular forces. This includes consideration for Johnson–Nyquist electrical–thermal and mechanical–thermal noise and flicker noise. The noise effective force is given by the ratio of the noise power to the force sensitivity, [74]:

$$F_{\text{NEF}} = \frac{\langle V_{\text{noise}}^2 \rangle}{\Delta V/F},$$

where $(\Delta V/F)$ is the force sensitivity of the cantilever and,

$$\langle V_{\text{noise}}^2 \rangle = \underbrace{\frac{24 k_{\text{B}} T L \rho}{wt}(f_{\text{max}} - f_{\text{min}})}_{\text{J–N electrical–thermal}} + \underbrace{\frac{2 \alpha V_{\text{bias}}^2}{8 L t w n} \ln\left(\frac{f_{\text{max}}}{f_{\text{min}}}\right)}_{\text{flicker}}$$

$$+ \underbrace{\frac{k_{\text{B}} T \, \Pi_{\text{l}}^2 L^2 K V_{\text{bias}}^2}{2 w^2 t^4 \omega_0 Q}(f_{\text{max}} - f_{\text{min}})}_{\text{J–N mechanical–thermal}}$$

Here L, w, and t are the length, width and thickness of the cantilever respectively; ñ is the piezoresistor resistivity; f_{max} and f_{min} are the maximum and minimum frequencies (bandwidth $B = f_{\text{max}} - f_{\text{min}}$); α is a dimensionless parameter; V_{bias} is the bias voltage; n is the carrier concentration; Π_{l} is the longitudinal piezoresistive coefficient; K is the cantilever stiffness; ω_0 is the natural frequency of the cantilever, and; Q is the quality factor. Note that the simpler formulation of thermal vibrations presented above for an AFM cantilever are still applicable.

As shown in Fig. 2, many of the micromechanical and microelectromechanical devices for cell mechanics to be described in "MEMS for Cell Mechanics" have yet to reach resolutions where thermal vibrations become limiting. This is largely due to the continued reliance on optical microscopy to measure displacements and external actuators. However, as these devices become more highly integrated with true MEMS sensing and actuation schemes, considerations for noise will again become paramount.

Complementary Imaging Techniques

All techniques reviewed here use optical microscopy in some capacity. The implementation may be conventional optical microscopy or could involve specialized techniques such as fluorescence or confocal microscopy for enhanced contrast and selective imaging. Typical (diffraction-limited) resolutions are on the order of hundreds of nanometers [75]. Note that the resolution refers to the ability to distinguish between an individual object and two closely-spaced objects. However the position of, for example, isolated fluorescent particles can be located with greater precision. In this case, positions are measured with reported precisions as great as a few nanometers [44]. This is aided by image processing to provide sub-pixel resolution. Ultimately, the goal of im-

plementing non-conventional microscopy techniques is to maximize contrast between features of interest and the background.

Fluorescence microscopy (FM) is widely used in cell mechanics studies to selectively image regions of interest on a cell [76]. Here fluorescent molecules (fluorophores) selectively bind to and label structures of interest. When illuminated with the proper wavelength, fluorophores absorb the incident light and emit a longer wavelength. Light from the sample is filtered by a dichroic mirror, allowing only the fluoresced light to reach the detector. In the resulting image, fluorescently-labeled regions appear bright in an otherwise black background. Common examples of FM in cell mechanics are the visualization of binding sites and cytoskeleton reorganization. The value of FM to biological studies is evidenced by the tremendous library of fluorophores and naturally-fluorescent gene products identified for virtually any component of living systems [76] (see [77] for libraries of fluorophores).

Confocal microscopy (CM) produces images with extremely reduced depth-of-focus, effectively giving cross-sectional views of the specimen [75, 78]. This is achieved using a point illumination source and a pinhole placed in front of the detector at the conjugate focal plane of the sample (the location at which the point source is re-focused to a point after passing through the objective lens). The pinhole blocks incident light that does not originate from the focal plane of the sample. Typical resolutions of commercially-available confocal microscopes are on the order of 200 nm [75]. CM, often performed in conjunction with FM, generally yields sharper images than those of FM alone due to the pinhole, which blocks background fluorescence. Multiple planar images may be reconstructed to create three-dimensional renderings of the specimen. Laser scanning confocal microscopy is a more recent form of CM. Here a laser source is scanned over the sample by a series of mirrors. As with CM, a pinhole rejects out-of-focus light. Each illuminated point captured represents a single pixel in a two- or three-dimensional image that is reconstructed by a computer [75].

Beyond imaging cells, microscope-based techniques have been demonstrated for studying cell dynamics, structure-function relationships, and even perturbing molecular function (for a review of these techniques, see [79]). For example, Chromophore Assisted Laser Inactivation (CALI) is used to perturb protein activity in cells. Here a chromophore-labelled antibody is used to target a protein of interest [79]. When exposed with the proper wavelength, the chromophore produces free radicals. These free radicals inactivate the targeted protein. In this way, CALI provides a high resolution, highly specific means of molecular perturbation without altering the cellular genetics.

While extremely effective in visualizing selected cellular components, methods of optical microscopy are not neces-

sarily immediately applicable to experimental cell mechanics. There is often a tradeoff between optimizing imaging conditions to quantify, for example, displacement of a bead, and obtaining the best possible visualization of the corresponding cell response. Similarly, as will be discussed later, many current MEMS devices rely on optical microscopy to simultaneously quantify deflection of compliant-beam force sensors and observe cell response. Future MEMS devices with greater sensor/actuator integration will reduce reliance on microscopy for force and displacement quantification, allowing greater optimization of cell imaging.

Further Motivation: Modeling Cell Mechanics

To further motivate advances in experimental techniques, we review model-based approaches to understanding the mechanics of cells, subcellular processes, and biomolecules. These models are often used to explain experimentally-observed cell responses, in some cases using experimentally-determined mechanical parameters. As previously mentioned, the range of relevant spatial and temporal scales complicates modeling efforts. With these models, we gain not only predictive power, but the ability to better understand the mechanisms that drive the phenomena observed in experiments.

A key challenge towards deciphering the structure-function paradigm for living cells is to interpret the response measured in the experiments outlined in "Common Experimental Techniques," as well as *in vivo* observations. The quest to address this challenge has yielded development of various theoretical and computational models for cells, subcellular components and biomolecules. These models have been used to complement the novel experiments designed for measuring material characteristics of cells, as well as to understanding certain behavioral aspects of living cells and states of human health and disease [80]. An example is the recent work on biomechanics of malaria-infected red blood cells, which has provided invaluable insight into the mechanisms of disease developments and alterations in the structural characteristics of red blood cells infected by the malaria parasite, *P. falciparum* [8, 81, 82]. Another example is application of biomechanical models in understanding infectivity and its connection to structure, as recently demonstrated for HIV particles [83]. In addition, the theoretical and computational models are strong tools for guiding experiments for probing certain aspects of behavior of living cells and their constituents. An example is a recent study on the mechanics of isolated nuclei in micropipette aspiration [84] and atomic force microscopy indentation [84, 85]. The developed computational model for an isolated nucleus, which distinguishes the structural role of major nuclear elements, revealed that the overall response of an isolated nucleus in micropipette aspiration is very sensitive to the nuclear lamina properties. This finding suggests that the micropipette aspiration exper-

iment can be used to effectively examine the influence of various alterations in the nuclear lamina, such as mutations in gene encoding lamin A and its bindings [84].

The theoretical models in the field of cell mechanics, range from scaling laws for cell adhesion [86] and qualitative models for cell mobility in two and three dimensions [87–89] to elastic rod models for protein-bound DNA loops [90] and detailed theoretical models which relate metabolic activity of red blood cells, through the consumption of ATP, to the stiffness and deformation of red blood cells in capillaries [81, 91]. Although these theoretical models have provided valuable insight into the mechanics of living cells, in general they cannot provide an accurate quantification of the material characteristics of living cells and subcellular components. This is mainly due to the heterogeneous and active structure of living cells, as well as the wide range of temporal and spatial scales involved in cellular processes.

The computational models in cell mechanics are generally classified to two main categories: Continuum-based approaches and Microscale approaches [80]. Microscale approaches have been used to interpret the response and behavior of cells, subcellular structures and their constituent biomolecules at various temporal scales. For example, tensegrity-based discrete models have been used to study various quantitative aspects of static and dynamic mechanical behavior of cells [38, 92–94]. At much smaller spatial scales, molecular dynamics simulations and Monte Carlo models have been developed for analyzing the response of biomolecules. The applications are broad and range from force-induced protein folding, unfolding and rupture [95–98] to understanding the effects of hyperglycemia on collagenolysis [99].

Continuum-based models in cell mechanics, and in general in biomechanics, are based on finite element methods. A key challenge in developing continuum-based computational models is choosing the material law capable of representing the behavior of distinct subcellular components under a complex state of stress, as well as their alterations due to biochemical, mechanical and electrical stimuli. The material laws incorporated in the computational models of cell mechanics vary from simple linear elasticity to 'active continua' models [100, 101], which account for the interplay of mechanics and biochemistry in regulating cell function, Fig. 3. This is further discussed in a complementary review article on continuum-based computational approaches in cell and nuclear mechanics [102]. The role of material and geometrical nonlinearity also can be incorporated easily in most computational models, which are of significant importance for certain applications. Examples are deformation of red blood cells in capillaries and cell motility where geometrical nonlinearly is of significant importance. While available computational techniques are capable of simulating and predicting many behavioral aspects of living cells

Fig. 3 Mechanical models proposed for single cell mechanics. A review of Liquid Drop models, which are mainly used to characterize the behavior of suspended cells, is provided in [82]. A review of the proposed Discrete models (also called Micro/nano structural models) is provided in Stamenovic and Ingber [166] and Ingber [167]
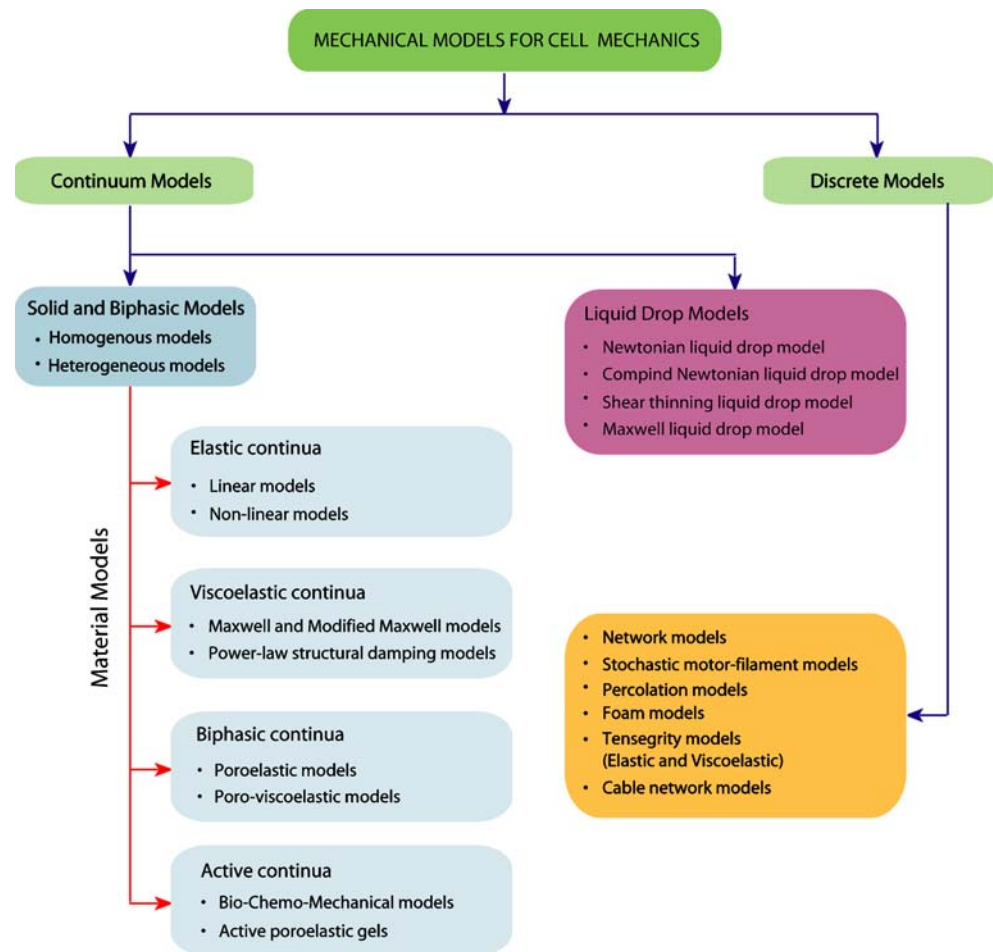
and subcellular components, still they fail to predict and simulate some of the important experimentally observed characteristics of cellular behavior. An example is focused propagation of mechanical stimuli applied to the cell membrane in the cytoskeleton [2, 103, 104]. A realization of this effect is the alteration of nuclear shape induced by pulling a microbead attached to the cell membrane. This 'action at a distance' effect can be predicted by novel computational models discussed by Wang and Suo [105] and Blumenfeld [106].

Cell function is regulated by complex interactions between biochemistry, biomechanics and genetics at spatial and temporal scales that extend over several decades. Development of multi-physics multiscale computational approaches which connect collective behaviors at different temporal and spatial scales can help immensely in furthering our knowledge of the structure-function paradigm in living cells. However, despite their importance, the application of these computational models is still in its infancy. The available multiscale computational approaches consist of hierarchical continuum-based models, hierarchical models based on microscale approaches, and models which bridge the length scales by combining continuum-based

models with microscale approaches. Hierarchical continuum-based models are mainly used to interconnect cell mechanics with collective tissue behavior such as for studying morphogenesis [107]. Hierarchical models based on microscale approaches have been also developed to study the mechanics of biomolecules as illustrated recently for mechanics and structure of collagens [98]. When a combination of continuum-based and microscale approaches are employed for interconnecting the behavior at different scales, coarse-graining of the local microscopic strain-stress relationships obtained from microscale approaches provides approximate continuum descriptions that can be applied at macroscopic levels. For example, network simulations of erythrocytes [108] can provide effective elastic constants of the membrane and the underlying filamentous structure, which then can be used for studying the overall deformation of red blood cells.

An interesting example of application of computational approaches is in understanding the complex mechanisms that regulate cell motility in two and three dimensions. These efforts have yielded development of various computational models, from continuum-based models based on finite element methods [109, 110] to stochastic models [89, 111] and

mutltiscale approaches [112, 113]. For example, the application of computational approaches in understanding tumor cell migration in 3D matrices has been recently demonstrated [114]. On the other hand, meso and molecular dynamics simulations were employed to study the making of ATP [115], the conformational states of Mg-ATP in water [116], and the mechanics and behavior of biomolecules involved in cell migration such as α-actinin [117].

Application of these theoretical and computational models for interpreting the response measured in various controlled experiments, have yielded various mechanical models for single cells (see Fig. 3) depending on the cell type and loading and experimental conditions. These models can be classified into two main categories: Continuum models and Discrete models. Liquid Drop models are widely used for characterizing the response of suspended cells [118, 119], while the adherent cells are generally modeled using homogenous or multi-layer Solid or Biphasic models. It is interesting to note that even for a single experiment and cell type, the model of choice could depend on the deformation level as discussed for the micropipette aspiration experiment on white blood cells by Lim et al. [82]. Most of the available models of adherent cells consider the cell as one homogenous material, in general representing the cytoskeleton, which considerably simplifies the analysis of experimental data. Mechanical models that account for the heterogeneous structure of the cell are critical for understanding certain aspects of cellular behavior such as the response to the localized perturbation applied to the cell membrane [120] or nuclear envelope [18].

MEMS for Cell Mechanics

As focus shifts from identifying cell-level responses to investigating the structure-function paradigm that drives them, the need for experimental techniques combining quantitative force and displacement transduction with simultaneous imaging of cellular components grows. MEMS hold the potential to meet these demands, providing the modeling community with highly repeatable results reflecting well-defined loading or deformation conditions while complementing existing experimental techniques. As will be discussed, the accessible force range of many of the MEMS-based systems extends to 100 s of nanoNewtons or greater. This is beyond the range of commonly-used magnetic and optical tweezers and many of the AFM probes. Cellular forces, which arise from cytoskeletal structures and the action of clusters of molecules (e.g., integrins), typically fall in the 10 s of nanoNewtons range or higher. For comprehensive study of mechanotransduction, forces of this range must be investigated in addition to those individual molecular forces already characterized by exiting techniques. Thus, we emphasize the complementary

as opposed to competitive relation of MEMS-based devices to existing techniques.

MEMS lend themselves naturally to cellular and subcellular level mechanical testing. Due to their intermediate size, MEMS serve as an excellent interface between our naturally macroscale tools and micro- or nano-scale biological systems. The well-established MEMS literature details numerous sensors and actuators exhibiting excellent performance characteristics. These sensing and actuation schemes will make possible self-sensing and actuating devices, eliminating the need for off-chip systems. The size and robustness of these devices creates the possibility of applying multiple independent sensors and actuators in cell-friendly environments. Furthermore, many of the MEMS-based sensing and actuation schemes scale favorably. For example, the time response, sensitivity, and power consumption of electrostatic displacement sensors improve as their dimensions shrink. Thus as devices are designed for finer scales, their performance improves.

Advantages of MEMS for cell mechanics are emergent in current MEMS devices, allowing accurate transduction of forces and displacements relevant at most levels of the hierarchical cell structure. A set of these devices representative of the current state of MEMS for cell mechanics is reviewed in this section. We consider a broad range of devices that leverage fabrication methods and operating principles of the well-established MEMS field. This includes devices that do not necessary have all components of a true "microelectromechanical" system. First, we review purely mechanical devices with compliant beams used to infer forces from optically-measured displacements via a known spring constant. These devices rely on external instruments for actuation. Next, fully microelectromechanical devices are reviewed. These devices begin to reduce reliance on external sensors and actuators. Later, MEMS sensors and actuators that have yet to be applied to study cell mechanics are discussed in terms of their potential to benefit the field.

Some of the devices reviewed are depicted schematically in Fig. 4. This figure highlights the reliance on microfabricated compliant beams, especially that of the purely mechanical micro-scale devices. In some cases, the beams simply confine motion to specific axes, replacing bearing or sliding contacts used in macro-scale devices. In others, the stiffness of the beams is calibrated such that measured displacements may be converted to forces. To compare their performance with other experimental techniques, the functional ranges of these devices are included in Fig. 2.

Micromechanical Devices: Pillars, Probes, and Pullers

Micro-scale pillars, probes and pullers have been used in a broad range of experiments in cell mechanics. These purely mechanical devices leverage well-established microfabrica-

Fig. 4 Schematic depiction of MEMS for cell mechanics emphasizing the use of compliant beams. The actuation in each device is depicted by an arrow. Δ denotes a displacement imposed by an external actuator. F_{comb}, F_{cell}, F_{app}, refer to forces imposed by an electrostatic comb-drive actuator, the cell, or other actuator respectively. F_{sense} denotes load measurement by optical imaging of beam deflection (note that they are not necessarily imaged at this location). Δ_{sense} denotes the measurement of displacement by optical microscope. See Table 2 for references for each device
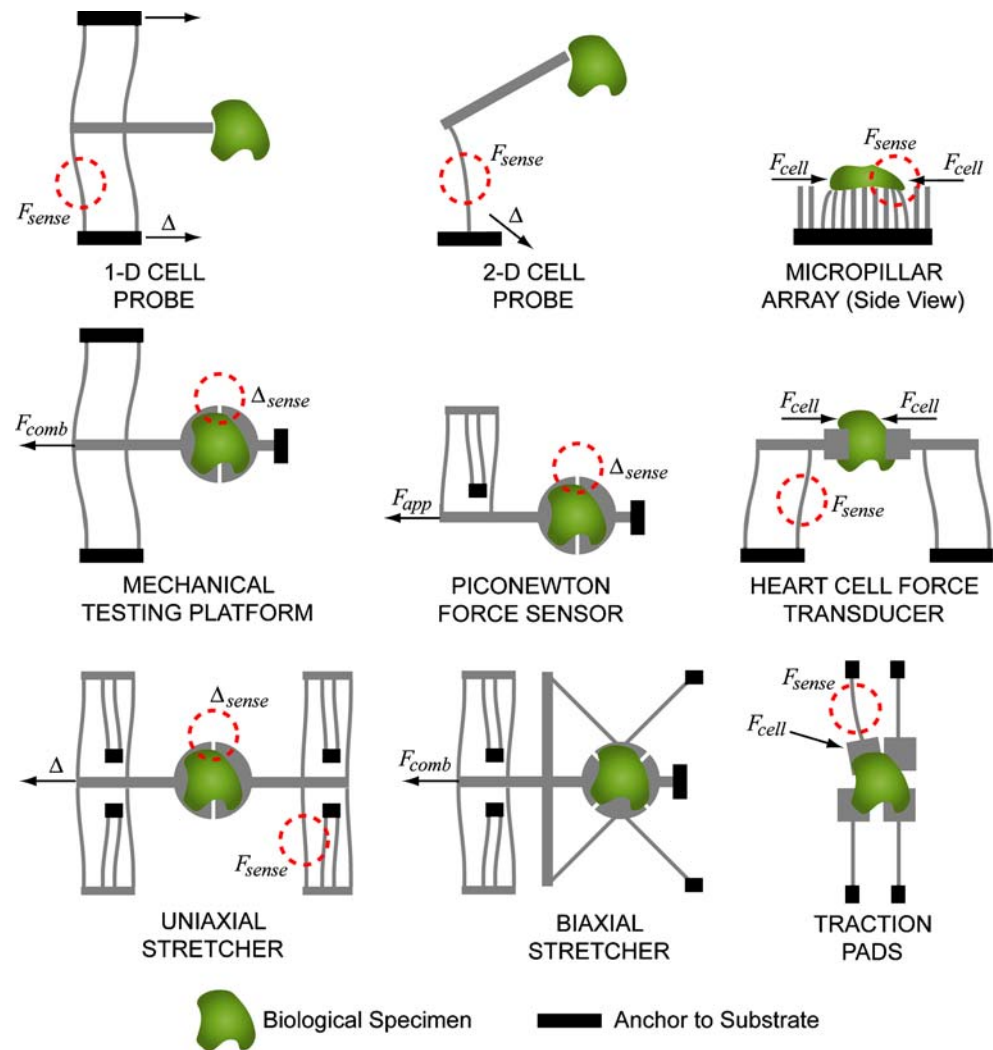
tion techniques to create systems with operational parameters relevant to the study of cell mechanics. The devices described in this section operate in conjunction with an optical microscope used to observe the deflection of compliant beams (see Fig. 4). In most cases, the stiffness of the beams is characterized, allowing optically-measured displacements to be converted to forces.

Arrays of closely-spaced compliant silicon or polymer pillars are used to study interactions between cells and their substrate [59–63]. The cell spreads across a bed of upright pillars, which deflect independently in response to local traction (see "Micropillar Array" in Fig. 4). This deflection is measured by optical microscopy and traction forces are estimated based on the calibrated stiffness of the pillars, each pillar yielding an independent force vector. Combined, these force vectors form a map of subcellular traction forces. A key advantage to this technique is the high number of independent force measurements provided by the pillars. The local substrate stiffness (stiffness of each pillar) can be varied across the substrate through the geometry of the pillars

[60]. Taking advantage of the large number of independent force measurements, these micropillar arrays enable a variety of novel studies. For example, by controlling adhesion to the pillars, Tan et al. demonstrated that traction forces are regulated by cell morphology [60]. In another application, Roure et al. showed that traction forces are greatest about the edge of epithelial cells [61]. Most recently, Sniadecki et al. embedded cobalt nanowires in the micropillars [63]. An externally-applied magnetic field was then used deflect the nanowire-containing pillars, while those without embedded nanowires acted as before to passively measure the resulting force response. With the added actuation capability, the authors observed local focal adhesion recruitment in response to step force inputs [63].

The pillars are made by casting poly(dimethylsiloxane) (PDMS) into a high-aspect-ratio mold or etching silicon. The compliance of the pillars is controlled through their geometry and the choice of material such that their deflection in response to cell traction is readily measured by optical microscopy yet small enough to prevent adjacent pillars from

contacting each other. The accuracy of this method is determined by the accuracy of the pillar stiffness estimates and, like many other methods, by the resolution of the optical displacement measurements. Before use, the PDMS is typically coated with fibronectin to promote adhesion. The tops of the pillars may be fluorescently labeled to improve imaging [61]. Rather than coating the entire device in fibronectin, the tops of the pillars may be selectively functionalized [60] by microcontact printing [64]. This helps prevent the cell from spreading down the sides of the pillars. If the cells do spread between the pillars, the force-deflection relationship for the calibrated pillars is no longer well-defined. While selective functionalization of the tops of the pillars reportedly reduces cell spreading between pillars, it is difficult to quantify the degree to which the fibronectin solution diffuses down the walls of the pillars upon printing. Furthermore, the effect of the discontinuous substrate on the cell response is unclear.

Saif and coworkers report a series of micromachined probes (see "1-D and 2-D Cell Probe" in Fig. 4) to investigate the force response of cells [121–123]. Each device consists of a probe suspended on a single or pairs of compliant beams of known stiffness. Pairs of beams confine the motion of the probe to a single axis. Use of a single beam allows the probe to move in the plane of the substrate, giving two-dimensional force readings. The entire probe-beam system is translated independently of the cell by a three-axis piezoelectric actuator to bring the probe into contact with the cell. By observing the deflection of the beams through an optical microscope, the applied force of the probe is calculated using the known spring constant of the beams. Beam calibration is performed by deflecting them against an AFM cantilever of known stiffness and comparing the magnitude of deformation. The probe can be functionalized with fibronectin, to promote adhesion [123]. This allows observation of the stretch response of cells by retracting the probe after adhesion. The resolution is limited by the resolution of the optics and uncertainties in the calibration of the beam spring constant.

Similar experiments to those performed by AFM were conducted using the cell probes. Use of the cell probes requires less complex equipment and simplifies imaging of the cell response as there is no AFM equipment to block the field of view. Note that biological AFMs are commercially available with inverted fluorescence microscopes beneath the sample. However, these can add significant cost to the already expensive AFM equipment. Using their micromachined probe, Saif and coworkers investigated morphological changes in cells in response to mechanical disturbances [121–123]. Both compressive and tensile forces were applied by functionalizing the probe to promote integrin activation. They demonstrated that probe indentation and retraction elicits a response by the actin network in GFP-actin transfected monkey

kidney fibroblasts [121]. The authors reported a hysteretic force response of the cells, which they attributed to observed actin agglomeration upon indentation.

Serrel et al. fabricated a micromechanical uniaxial puller (see Fig. 4) to apply well-defined tensile loading to adherent cells [124]. The device consists of a platform which is split down the center and coated with fibronectin to promote adhesion. A single cell is allowed to adhere across the two halves of the platform. One half of the platform is then pulled away from the other using a probe station to strain the cell. The probe station is capable of significantly larger displacements than typical MEMS-based actuation schemes, allowing for complete de-adhesion experiments. The opposite half of the platform is linked to the substrate by a series of compliant beams which act as load sensors. The deflection of these beams is imaged by high-speed camera then used to compute the applied force by the known spring constant. Using digital image processing, displacement resolutions of 50 nm were reported. Addition of a MEMS differential capacitive load sensor (see for example [125, 126]) could eliminate the need for this optical measurement in the future.

The uniaxial puller was used to characterize the force-displacement response of individual fibroblasts [124]. The initial response was linear. However, the onset of de-adhesion resulted in nonlinear behavior as individual adhesion sites failed. Complete loss of adhesion occurred at over 1500 nN, which is significantly higher than de-adhesion forces reported elsewhere. The authors attributed this discrepancy to the extensive fibronectin coating and high surface roughness of the platform as compared to the relatively smooth substrates used in other experiments.

Sheetz et al. demonstrated a micromachined substrate (see "Traction Pads" in Fig. 4) used to measure traction forces generated by fibroblasts [127]. The substrate contains a large array of square pads, each fixed to the free end of a cantilever beam (in the plane of the substrate) hidden beneath the surface. Much like the micropillar arrays, these cantilevers bend in response to traction forces applied to the pads by migrating cells. A camera tracks the motion of the pads and images are later processed to determine the corresponding force using the known spring constant of the cantilever beams. In this case, the deflection of the cantilevers depends not only on the magnitude of the traction, but also on the angle of this vector with respect to the cantilever (the deflection of the cantilever for a given force is greatest when the force is perpendicular to the cantilever and minimal when the force is parallel to the cantilever). To resolve this issue, the authors assumed the force to be along the long axis of the cell [127] as it was shown that tractions generated by fibroblasts are directed primarily along this axis [128]. The validity of this assumption, along with the calibration of the beams and resolution of the optics, determines the accuracy of the measurements produced in this

experiment. Using this device, Sheetz et al. observed intermittent rearward facing forces at the front of migrating fibroblasts and larger forward-directed forces at the tail [127]. Based on these observations of dorsal and ventral traction forces, the authors propose a mechanism for fibroblast movement; namely that fibroblasts continually generate new adhesive contacts at the front and release contacts at the rear.

Lin et al. investigated the contraction of living heart muscle cells using a micromechanical force transducer [129] (see "Heart Cell Force Transducer" in Fig. 4). As with many of the other devices, this uses calibrated compliant beams as load sensors. The heart cell is fixed between two sets of polysilicon clamps, each suspended by a pair of flexible beams. The effect of the clamps on the natural behavior of the cell is unclear. Again, the uncertainty of the beam calibration and the resolution of the optical system determine the resolution of the device. Using this device, the authors measured the maximum force, maximum force per unit area, and the dependence of the percentage of maximum force on the calcium concentration of the solution. Here physiologically-representative forces could not be generated in this device due to the high compliance of the beams required for optically-measurable deflections. This demonstrates the value of fully microelectromechanical sensors. To remedy this, the authors propose use of MEMS strain gauges on the beams to eliminate the optical imaging and allow for stiffer beams, as well as microactuator integration for more advanced studies [129].

A MEMS platform was fabricated to study the effects of mechanical tension on cerebral cortex neurogenesis [130, 131]. The device consists of a clamp-and-ratchet microstructure used to grip a compliant PDMS membrane and stretch it. The tissue is cultured on the PDMS membrane. One end of the membrane is fixed to the substrate while the other end is gripped by the clamp. The clamp is then pulled and the ratchet mechanism holds it at pre-set increments of strain. The resulting neuronal migration is then observed. To the best of our knowledge, the device has yet to be fully implemented, though preliminary studies showed embryonic brain tissue and neurospheres cultured on PDMS survived under tension for several days.

A MEMS-based piconewton force sensor was reported (see "Piconewton Force Sensor" in Fig. 4, Table 2) [132]. This sensor works with compliant beams similar to those of other devices. Deflection is measured using integrated gratings by an optical microscope. The device was used to characterize individual magnetic beads as well as to map the magnetic field of an electromagnet. The device may be used to more accurately calibrate the magnetic beads used in the magnetic methods described in "Motivation for Use of MEMS." While not yet implemented in cell mechanics studies, the authors suggest its applicability for these studies

Table 2 Selected references for Figs. 2 and 4

	Technique	References
Conventional	Micropipette aspiration	[13]
	AFM	[15–17, 19–22, 85]
	Optical/laser trapping	[8, 12, 24–30]
	Magnetic beads	[12, 34–36]
	Compliant substrates	[53–58]
MEMS-based	1-D and 2-D cell probe	[121–123]
	Mechanical testing platform	[133]
	Uniaxial stretcher	[124]
	Micropillar arrays	[59–63]
	Heart cell force transducer	[129]
	Traction pads	[127]
	Microfabricated cantilevers	[165]
	Bi-axial stretcher	[134]
	Piconewton force sensor	[132]

The last two devices have been demonstrated in the literature and cite their application to cell mechanics. However, to the best of our knowledge, they have yet to report results of such tests.

due to its extremely fine force/displacement resolution. Furthermore, operation in both air and water was demonstrated, making it attractive for use in cell-friendly fluid environments.

The micromechanical devices described above leverage the fabrication techniques of the MEMS industry to create highly-scaled devices. As shown in Fig. 2, their performance characteristics are equivalent to or approaching many existing experimental techniques for cell-level studies. Active devices like the cell stretchers impose well-defined loading conditions, minimizing assumptions and computational expense. At the same time, the lack of an electrical component requires continued reliance on external actuators and sensors such as optical microscopes that limit the resolution. Accordingly, these devices have yet to reach the resolutions required for single-molecule investigations. Furthermore, reliance on large-scale external devices limits the possibilities for incorporating large numbers of independent elements on a single device. Finally, reliance on an optical microscope requires imaging conditions conducive to quantifying, for example, deflection of a beam. Accordingly, imaging conditions may not be fully optimized for observing the cell response.

Microelectromechanical Systems for Cell Mechanics

The microelectromechanical systems for cell mechanics reviewed here have the added advantage of on-chip actuators over the above micromechanical devices. While a limited number of these devices have been demonstrated, the benefits are readily apparent. As will be described in "Further Potential Applications of MEMS to Cell Mechanics Studies,"

increased sensor/actuator integration will bring the resolution of these devices in line with other experimental techniques, while maintaining the advantages of multiple probe-cell interactions, limited reliance on external systems, well-defined loading conditions, and cell-friendly environments.

Eppell et al. fabricated an electrostatically-actuated MEMS mechanical testing platform to determine the mechanical properties of hydrated collagen fibrils [133]. The fibril specimen is bonded across the gap between a fixed and a moveable pad using epoxy. An electrostatic comb-drive actuator pulls the moveable pad, loading the specimen in pure tension. The motion of the pad is constrained to a single axis by compliant tether beams (see "Mechanical Testing Platform" in Fig. 4). The force produced by the comb-drive actuator was calibrated using the voltage-displacement response of the device without a specimen mounted and the stiffness of the beams (calculated by finite element analysis). The resulting displacement was measured by observing an integrated Vernier scale with an optical microscope, yielding a displacement resolution of 0.25 μm. Force-displacement curves for the fibril samples were obtained by subtracting the device response without the sample from the response with the fibril sample mounted. Though not executed, the authors [133] suggest the use of fluorescently tagged antibodies to provide punctate staining and visualization of local strain distribution.

Using the MEMS mechanical testing platform, Eppell et al. measured the force-displacement (and corresponding true stress-Almansi strain) response of axially-loaded fibrils [133]. From this data, they reported nominal values of secant moduli for both small and large strains. For comparison, they also calculated the modulus based on the resonant frequency of the device with and without the fibril attached. This value of 0.53 GPa agreed well with the statically-determined modulus. The electrostatic actuator used in the mechanical testing platform has the added advantage of allowing sample fatigue by cyclic loading. This cyclic loading may be super-imposed on a nominal stress with the simple addition of an AC input to the DC bias on the actuator. With cyclic loading, the authors found a monotonically decreasing modulus with increasing numbers of cycles and successively higher rates [133].

A MEMS biaxial puller was fabricated to impose a well-defined state of uniform biaxial stress on the cell [134]. Like the uniaxial puller (see "Micromechanical Devices: Pillars, Probes, and Pullers"), the cell adheres to a split platform. In this case, the platform is divided into four rather than two equal pieces. Upon actuation by an electrostatic comb-drive actuator, the four pieces separate directly away from each other on a set of micromachined linkages. To the best of our knowledge, operation of the device with a live cell has yet to be reported. Nonetheless, this device eliminates the need for an external actuator and preliminary results show nearly ideal biaxial strain. The authors suggest alternative actuators, including thermal, magnetic, or piezoelectric schemes. In this case, they selected the comb-drive for its high accuracy and speed, low power consumption and cost to fabricate, and moderate driving voltage [134].

Capacitive load or displacement sensors are commonly used in a broad range of MEMS devices. For example, Zhu et al. demonstrated nanonewton resolution in a differential capacitive load sensor used for tensile tests of one-dimensional nanostructures such as carbon nanotubes and nanowires [125, 126]. Sun et al. fabricated a multi-axis capacitive load sensor for cellular force sensing [135]. The device consists of a probe fixed at one end to transverse sets of high-aspect-ratio electrostatic comb drive structures that sense probe forces in two dimensions. This eliminates the need for optically-measured deflection of beams for load sensing. Furthermore, the broad operating range, which spans from tens of nanonewtons to hundreds of micro-newtons (10^{-8}–10^{-4} N), allows for a diverse set of experiments with a single device. The authors cite intended applications to cell mechanics including force feedback for robot cell positioning, modeling of membrane properties for cell injury and recovery studies, and DNA injection embryo pronuclei. This device could potentially be integrated into many of the previously-described probe devices to replace the optical displacement measurements. Furethermore, the use of electrostatic combs present the possibility that this device could be used as an actuator as well as a sensor.

The devices described here demonstrate some of the potential of MEMS for advancing studies of cell mechanics. By incorporating electrical-mechanical transduction, these devices reduce reliance on external tools. For example, simple electrical input in the form of a DC signal could then be used to control applied cell stimulus. Likewise, true MEMS sensors output a simple electrical signal. But while promising, the application of MEMS to cell mechanics is relatively new. Accordingly, devices incorporating combinations of multiple MEMS sensors and actuators have yet to be demonstrated.

Further Potential Applications of MEMS to Cell Mechanics Studies

To date, MEMS devices for cell mechanics incorporate a limited number of the available MEMS sensors and actuators, yet they enable novel experiments in force ranges not attainable by other common techniques. The next generation of MEMS for cell mechanics will enable investigations on multiple levels through combinations of multiple sensors and actuators, while maintaining a cell-friendly environment to minimize collateral impact on natural cell processes. Cell response will continue to be imaged by optical microscopy under optimal conditions, while forces and displacements

are *independently* transduced through a simple electrical interface.

By incorporating on-chip MEMS sensors and actuators, devices gain the ability to produce and sense their own motion and forces. This reduces reliance on external devices, simplifying the experimental setup and allowing for smaller devices better matched to the dimensions of the samples they interrogate. For example, sub-attogram mass detection has been demonstrated in environmental conditions using self-sensing piezoresistive cantilevers, suggesting the possibility of sub-piconewton force sensing without the conventional optical-electrical AFM detection system [136]. For an excellent review of MEMS sensors and actuators and detailed comparison of their performance characteristics, see [137].

Force- and displacement-controlled actuators

The ability to prescribe force or displacement independently of cellular response allows direct characterization of a range of cell properties. For example, displacement-controlled actuators, which produce a prescribed displacement regardless of the required force (within a functional range), offer the unique ability to capture the onset of nonlinearities including softening or individual bond rupture during straining. These events often occur too rapidly to be accurately characterized with force-controlled actuators where, for example, strain jumps suddenly with the occurrence of such an event. Displacement-controlled actuators prevent this sudden yielding. Force-controlled actuators supply a prescribed force, regardless of the required displacement (again within a functional range). MEMS electrostatic actuators are a common example of force-controlled actuators as they produce a force for a given voltage input.

MEMS thermal [125, 138] and piezoelectric [139] actuators are common examples of displacement-controlled schemes. Thermal actuators have demonstrated nanometer resolution in mechanical testing of nanowires, carbon nanotubes, and ultra-thin films [125, 126, 138]. Piezoelectric actuators have proven capable of accurately prescribing displacements over many orders of magnitude (angstroms to tens or hundreds of microns) in AFM. Active piezoelectric cantilevers have been used in place of common passive AFM cantilevers as they are both self-sensing and self-actuating (see for example [74, 140]). Microfabrication techniques allowing incorporation of piezoelectric elements in MEMS are now available. For example, piezoelectric thin films are deposited by physical vapor deposition [141] or spin-coating [142] then patterned by reactive ion etching or soft lithography [143]. These techniques combine to enable highly compact, highly integrated devices. By eliminating large external actuators and integrating on-chip piezoelectric elements, multiple elements can be actuated or sensed, all interacting with the cell independently. A major advantage is their ability to act both as sensors and actuators without modification, meaning an element can at one time be used as an actuator and later as a sensor.

Electroactive or conjugated polymers can be used similarly to conventional piezoelectric materials [144–146]. Electroactive polymers, such as polypyrrole, can be electrochemically deposited [144]. Piezoelectric polymer thin films, such as polyvinylidene fluoride (PVDF), are also of interest [147]. Unique advantages of electroactive polymers include their large strain capabilities (for linear, volumetric, and bending actuation) and their ability to operate in liquid electrolytes [145]. These are currently being investigated for actuators in "cell clinic" chips for single-cell studies [145, 146].

A common difficulty in testing global properties of some cells is their propensity for large deformations. These displacements are difficult to produce with the limited travel of most common MEMS actuators. Several large-displacement MEMS actuators have demonstrated potential to overcome this limitation. These include scratch drives [148] and inchworm actuators [149]. For example, Bronson et al. [150] propose a device using a scratch drive actuator to apply tensile loading and large deformation to cells. Here the cell is fixed to a platform similar to that of the uniaxial puller described in "Micromechanical Devices: Pillars, Probes, and Pullers." The scratch drive provides the required large displacements. Corresponding load is sensed by a folded beam separating the actuator from the cell platform [150].

Tailoring the cell environment

Cells are highly sensitive to their environment and thus special care must be taken when interpreting results obtained while exposing the cell to unnatural conditions. Alterations to the cell's environment can cause loss of natural functions and dedifferentiation [151]. The method of culture largely determines cell environment. For example, cells may grow as a dense monolayer, in which case they have familiar neighboring cells in the lateral directions but not above or beneath them. Alternatively, individual cells or aggregates may form within a collagen gel or small numbers may interact with features in the substrate surface [152]. Even methods that do in fact create a three-dimensional culture generally do not exhibit homogeneous cell morphology, local matrix properties, or cell polarity [152].

Using microfabrication techniques, conditions may be tailored to create a more natural environment for the cell. Dusseiller et al. microfabricated single-cell-sized wells on a silicon substrate [152]. The walls and bottom of each well were functionalized with fibronectin while other surfaces were coated in PEG-*graft*-copolymer to make them noninteractive. This resulted in single-cell micro-three-dimensional

cultures, allowing tight control over cell shape and surface functionalization. Additionally, phospholipids can be assembled with high resolution by techniques such as dip-pen nanolithography [153] to mimic biological membranes [154].

The ability to operate on-chip sensors and actuators in aqueous solutions simplifies maintenance of a natural cell environment. Some MEMS sensors and actuators, such as electrostatic and thermoelectric actuators, have proven effective in aqueous environments [155, 156]. Here electrostatic actuators are operated with AC rather than DC to avoid electrolysis with the surrounding fluid. Those that cannot operate in fluid may be positioned outside the fluid region and interact with extended micromachined probes.

Concluding Remarks

Existing experimental and modeling techniques continuously provide new insight into the underlying mechanisms driving observed phenomena in cell mechanics. Here we summarized these techniques in the context of motivating the next generation of complementary MEMS-based devices for studies of cell mechanics. MEMS will clearly not replace existing techniques which already exhibit extremely fine force and displacement resolutions. However, the use of self-sensing, self-actuating MEMS will reduce reliance on external equipment, allowing conditions to be optimized for imaging the cellular response. The small size of these devices will allow well-defined independent force- or displacement-controlled stimuli and collection of rich data sets from multiple points on the cell in the form of simple electrical input/output. Furthermore, conditions will be tailored to better match natural cell environments. While issues remain regarding implementation, MEMS offer great promise for the next generation of novel experiments in cell mechanics. In this light, we view MEMS-based devices as complementary tools to existing techniques, enabling comprehensive study of cell mechanics and mechanotransduction. The extremely fine force and displacement resolutions of existing techniques allow interrogation of single molecule systems, while MEMS extend the investigation to the cellular level.

References

1. Zhu C, Bao G, Wang N (2000) Cell mechanics: mechanical response, cell adhesion, and molecular deformation. Annu Rev Biomed Eng 02:189–226.
2. Maniotis A, Chen C, Ingber D (1997) Demonstration of mechanical connections between integrins, cytoskeletal filaments, and nucleoplasm that stabilize nuclear structure. PNAS 97:849–854.
3. Ingber D (1997) Tensegrity: The architectural basis of cellular mechanotransduction. Annu Rev Physiol 57:575–599.
4. Engler A, Sen S, Sweeney H, Discher D (2006) Matrix elasticity directs stem cell lineage specification. Cell 126:677–689.
5. Chicurel M, Chen C, Ingber D (1998) Cellular control lies in the balance of forces. Curr Opin Cell Biol 10:232–239.
6. Discher D, Janmey P, Wang Y-L (2005) Tissue cells feel and respond to the stiffness of their substrate. Science 310:1139–1143.
7. Huang H, Kamm R, Lee R (2004) Cell mechanics and mechanotransduction: pathways, probes, and physiology. Am J Physiol Cell Physiol 287:C1–C11.
8. Suresh S, Spatz J, Mills J, Micoulet A, Dao M, Lim C, Beil M, Seufferlein T (2005) Connections between single-cell biomechanics and human disease states: gastrointestinal cancer and malaria. Acta Biomaterialia 1:15–30.
9. Shelby J, White J, Ganesan K, Rathod R, Chiu D (2003) A microfluidic model for single-cell capillary obstruction by *Plasmodium falciparum*-infected erythrocytes. PNAS 100:14618–14622.
10. Kamm R, Kaazempur-Mofrad M (2004) On the molecular basis for mechanotransduction. Mechanics and Chemistry of Biosystems 1:201–210.
11. Bao G, Suresh S (2003) Cell and molecular mechanics of biological materials. Nature Materials 2:715–725.
12. Van Vliet KJ, Bao G, Suresh S (2003) The biomechanics toolbox: experimental approaches for living cells and biomolecules. Acta Mater 51:5881–5905.
13. Hochmuth RM (2000) Micropipette aspiration of living cells. J Biomech 33:15–22.
14. Rand R, Burton A (1964) Mechanical properties of the red cell membrane. Biophys J 4:115–135.
15. Mahaffy R, Park S, Gerde E, Kas J, Shih C (2004) Quantitative analysis of the viscoelastic properties of thin regions of fibroblasts using atomic force microscopy. Biophys J 86:1777–1793.
16. Radmacher M (2002) Measuring the elastic properties of living cells by the atomic force microscope. Atomic Force Microscopy in Cell Biology 68:67–90.
17. Charras G, Lehenkari P, Horton M (2001) Atomic force microscopy can be used to mechanically stimulate osteoblasts and evaluate cellular strain distributions. Ultramicroscopy 86:85–95.
18. Vaziri A, Lee H, Kaazempur-Mofrad M (2006) Deformation of the nucleus under indentation: mechanics and mechanisms. J Mater Res 21:2126–2135.
19. Panorchan P, George J, Wirtz D (2006) Probing intermollecular interactions between vascular endothelial cadherins pairs at single-molecule resolution and in living cells. J Mol Biol 358:665–674.
20. Panorchan P, Thompson M, Davis K, Tseng Y, Konstantopoulos K, Wirtz D (2006) Single-molecule analysis of cadherin-mediated cell-cell adhesion. J Cell Sci 119:66–74.
21. Florin E-L, Moy V, Gaub H (1994) Adhesion forces between individual ligand-receptor pairs. Science 264:415–417.
22. Hyonchol K, Arakawa H, Osada T, Ikai A (2002) Quantification of fibronectin and cell surface interactions by AFM. Colloids Surf B Biointerfaces 25:33–43.
23. Mathur A, Trusky G, Reichert W (2000) Atomic force and total internal reflection fluorescence microscopy for the study of force transmission in endothelial cells. Biophys J 78:1725–1735.
24. Hochmuth RM, Shao J-Y, Dai J, Sheetz M (1996) Deformation and flow of membranes into tethers extracted from neuronal growth cones. Biophys J 70:359–369.
25. Dai J, Sheetz M (1995) Mechanical properties of neuronal growth cone membranes studied by tether formation with laser optical tweezers. Biophys J 68:988–996.
26. Dai J, Ting-Beall H, Sheetz M (1997) The secretion-coupled endocytosis correlates with membrane tension chances in RBL 2H3 cells. J Gen Physiol 110:1–10.
27. Dao M, Lim CT, Suresh S (2003) Mechanics of the human red blood cell deformed by optical tweezers. J Mech Phys Solids 51:2259–2280.

28. Henon S, Lenormand G, Richert A, Gallet F (1999) A new determination of the shear modulus of the human erythrocyte membrane using optical tweezers. Biophys J 76:1145–1151.

29. Lim CT, Dao M, Suresh S, Sow CH, Chew KT (2004) Large deformation of living cells using laser traps. Acta Mater 52: 1837–1845.

30. Mills JP, Qie L, Dao M, Lim CT, Suresh S (2004) Nonlinear elastic and viscoelastic deformation of the human red blood cell with optical tweezers. Mechanics and Chemistry of Biosystems 1:169–180.

31. Svoboda K, Block S (1994) Biological applications of optical forces. Annu Rev Biophys Biomol Struct 23:247–285.

32. Mehta A, Rief M, Spudich J, Smith D, Simmons R (1999) Single-molecule biomechanics with optical methods. Science 283:1689–1695.

33. Wen J-D, Manosas M, Li P, Smith S, Bustamante C, Ritort F, Tinoco I (2007) Force unfolding kinetics of RNA using optical tweezers. I. Effects of experimental variables on measured results. Biophys J 92:2996–3009.

34. Bausch AR, Ziemann F, Boulbitch AA, Jacobson K, Sackmann E (1998) Local measurements of viscoelastic parameters of adherent cell surfaces by magnetic bead microrheometry. Biophys J 75:2038–2049.

35. Haber C, Wirtz D (2000) Magnetic tweezers for DNA micromanipulation. Rev Sci Instrum 71:4561–4570.

36. Alenghat F, Fabry B, Tsai K, Goldmann W, Ingber D (2000) Analysis of cell mechanics in single vinculin-deficient cells using a magnetic tweezer. Biochem Biophys Res Commun 277:93–99.

37. Chen J, Fabry B, Schiffrin E, Wang N (2001) Twisting integrin receptors increases endothelin-1 gene expression in endothelial cells. Am J Physiol Cell Physiol 280:C1475–C1484.

38. Wang N, Butler J, Ingber D (1993) Mechanotransduction across the cell surface and through the cytoskeleton. Science 260:1124–1127.

39. Masksym G, Fabry B, Butler J, Navajas D, Tschumperlin D, Laporte J, Fredberg J (2000) Mechanical properties of cultured human airway smooth muscle cells from 0.05 to 0.4 Hz. J Appl Physiol 89:1619–1632.

40. Nollmann M, Stone M, Bryant Z, Gore J, Crisona N, Hong S-C, Mitelheiser S, Maxwell A, Bustamante C, Cozzarelli N (2007) Multiple modes of Escherichia coli DNA gyrase activity revealed by force and torque. Nature Structural and Molecular Biology 14: 264–271.

41. Oroszi L, Galajda P, Kirei H, Bottka S, Ormos P (2006) Direct measurement of torque in an optical trap and its application to double-strand DNA. Phys Rev Lett 97:058301.

42. Trimmer W (1989) Microrobots and micromechanical systems. Sens Actuators 19:267–287.

43. Crick F, Hughes A (1950) The physical properties of cytoplasm: a study by means of the magnetic particle method, Part I. Experimental. Exp Cell Res 1:37–80.

44. Tseng Y, Kole T, Wirtz D (2002) Micromechanical mapping of live cells by multiple-particle-tracking microrheology. Biophys J 83:3162–3176.

45. Dong C, Lei X (2000) Biomechanics of cell rolling: shear flow, cell-surface adhesion, and cell deformability. J Biomech 33:35–43.

46. Levesque M, Nerem R, Sprague E (1990) Vascular endothelial cell proliferation in culture and the influence of flow. Biomaterials 11:702–707.

47. Basso N, Heersche J (2002) Characteristics of in vitro osteoblastic cell loading models. Bone 30:347–351.

48. Trepat X, Grabulosa M, Puig F, Maksym G, Navajas D, Farre R (2004) Viscoelasticity of human alveolar epithelial cells subjected to stretch. Am J Physiol Lung Cell Mol Physiol 287:1025–1034.

49. Trepat X, Puig F, Gavara N, Fredberg J, Farre R, Navajas D (2006) Effect of stretch on structural integrity and microme-chanics of human alveolar epithelial cell monolayers exposed to thrombin. Am J Physiol Lung Cell Mol Physiol 290:L1104–L1110.

50. Geerts H, De Brabander M, Nuydens R, Geuens S, Moeremans M, De Mey J, Hollenbeck P (1987) Nanovid tracking: a new automatic method for the study of mobility in living cells based on colloidal gold and video microscopy. Biophys J 52:775–782.

51. Daniels B, Masi B, Wirtz D (2006) Probing single-cell micromachines in vivo: the microrheology of C. elegans developing embryos. Biophys J 90:4712–4719.

52. Yamada S, Wirtz D, Kuo S (2000) Mechanics of living cells measured by laser tracking microrheology. Biophys J 78:1736–1747.

53. Burton K, Park J, Taylor D (1999) Keratocytes generate traction forces in two phases. Mol Biol Cell 10:3745–3769.

54. Burton K, Taylor D (1997) Traction forces of cytokinesis measured with optically modified elastic substrata. Nature 385:450–454.

55. Lo C-M, Wang H-B, Dembo M, Wang Y-L (2000) Cell movement is guided by the rigidity of the substrate. Biophys J 79:144–152.

56. Beningo K, Wang Y-L (2002) Flexible substrata for the detection of cellular traction forces. Trends Cell Biol 12:79–84.

57. Beningo K, Wang Y-L (2002) Flexible polyacrylamide substrates for the analysis of mechanical interactions at cell-substrate adhesions. Methods Cell Biol 69:325–339.

58. Munevar S, Wang Y-L, Dembo M (2001) Traction force microscopy of migrating normal and H-ras transformed 3T3 fibroblasts. Biophys J 80:1744–1757.

59. Zhao Y, Zhang X (2006) Cellular mechanics study in cardiac myocytes using PDMS pillars array. Sens Actuators A 125:398–404.

60. Tan J, Tien J, Pirone D, Gray D, Bhadriraju K, Chen C (2003) Cells lying on a bed of microneedles: an approach to isolate mechanical force. PNAS 100:1484–1489.

61. Roure O, Saez A, Buguin A, Austin R, Chavrier P, Silberzan P, Ladoux B (2005) Force mapping in epithelial cell migration. PNAS 102:2390–2395.

62. Petronis S, Gold J, Kasemo B (2003) Microfabricated force-sensitive elastic substrates for investigation of mechanical cell-substrate interactions. J Micromechanics Mircoengineering 13:900–913.

63. Sniadecki N, Anguelouch A, Yang M, Lamb C, Liu Z, Kirschner S, Liu Y, Reich D, Chen C (2007) Magnetic microposts as an approach to apply forces to living cells. PNAS 104:14553–14558.

64. Xia Y, Whitesides G (1998) Soft lithography. Annu Rev Mater Sci 28:153-184.

65. Dike L, Chen C, Mrksich M, Tien J, Whitesides G, Ingber D (1999) Geometric control of switching between growth, apoptosis, and differentiation during angiogenesis using micropatterned substrates. In Vitro Cell Dev Biol 35:441–448.

66. Cavalcanti-Adam E, Volberg T, Micoulet A, Kessler H, Geiger B, Spatz J (2007) Cell spreading and focal adhesion dynamics are regulated by spacing of integrin ligands. Biophys J 92:2964–2974.

67. Gabrielson T (1993) Mechanical-thermal noise in micromachined acoustic and vibration sensors. IEEE Trans Electron Devices 40:903–909.

68. Rocha L, Cretu E, Wolffenbuttel R (2005) Measuring and interpreting the mechanical-thermal noise spectrum in a MEMS. J Micromechanics Mircoengineering 15:S30–S38.

69. Johnson JB (1928) Thermal agitation of electricity in conductors. Phys Rev 32:97.

70. Nyquist H (1928) Thermal agitation of electric charge in conductors. Phys Rev 32:110–113.

71. Mamin H, Rugar D (2001) Sub-attonewton force detection at millikelvin temperatures. Appl Phys Lett 79:3358–3360.

72. Yamada H, Kobayashi K (2007) Dynamic force microscopy for molecular-scale investigations of organic materials in various

environments. In: Bhushan B, Kawata S (eds) Applied scanning probe methods, vol. VI. Springer, pp 205–245.

73. Gittes F, Schmidt C (1998) Thermal noise limitations on micro-mechanical experiments. Eur Biophys J 27:75–81.

74. Villanueva G, Montserrat J, Perez-Murano F, Rius G, Bausells J (2004) Submicron piezoresistive cantilevers in a CMOS-compatible technology for intermolecular force detection. Microelectron Eng 73–74:480–486.

75. Prasad V, Semwogerere D, Weeks E (2007) Confocal microscopy of colloids. J Phys Condens Matter 19:113102.

76. Lichtman J, Conchello J-A (2005) Fluorescence microscopy. Nature Methods 2:910–919.

77. http://probes.invitrogen.com/handbook/. The handbook—a guide to fluorescent probes and labeling technologies, tenth edition. Invitrogen Corp.

78. Semwogerere D, Weeks E (2005) Confocal microscopy. In: Encyclopedia of biomaterials and biomedial engineering. Taylor and Francis, New York.

79. Roy P, Rajfur Z, Pomorski P, Jacobson K (2002) Microscope-based techniques to study cell adhesion and migration. Nat Cell Biol 4:E91–E96.

80. Vaziri A, Gopinath A (in press) Computational approaches in cell and biomolecular mechanics.

81. Gov N, Safran S (2005) Red blood cell membrane fluctuations and shape controlled by ATP-induced cytoskeletal defects. Biophys J 88:1859–1874.

82. Lim C, Zhou E, Quek S (2006) Mechanical models for living cells—a review. J Biomech 29:195–216.

83. Kol N, Shi Y, Tsitov M, Barlam D, Shneck R, Kay M, Rousso I (2007) A stiffness switch in HIV. Biophys J 92:1777–1783.

84. Vaziri A, Mofrad M (2007) Mechanics and deformation of the nucleus in micropipette aspiration experiment. J Biomech 40:2053–2062.

85. Vaziri A, Lee H, Mofrad M (2006) Deformation of the cell nucleus under indentation: Mechanics and mechanisms. J Mater Res 21:2126–2135.

86. Curvelier D, Théry M, Chu Y, Dufour S, Thiéry J, Bornens M, Nassoy P, Mahadevan L (2007) The universal dynamics of cell spreading. Curr Biol 17:694–699.

87. Mogilner A, Edelstein-Keshet L (2002) Regulation of actin dynamics in rapidly moving cells: a quantitative analysis. Biophys J 83:1237–1258.

88. DiMilla P, Barbee K, Lauffenburger D (1991) Mathematical model for the effects of adhesion and mechanics on cell migration speed. Biophys J 60:15–37.

89. Dickinson R, Tranquillo R (1993) A stochastic model for adhesion-mediated cell random motility and haptotaxis. J Math Biol 31:563–600.

90. Balaeff A, Mahadevan L, Schulten K (2006) Modeling DNA loops using the theory of elasticity. Phys Rev E 73:031919.

91. Gov N (2007) Active elastic network: cytoskeleton of the red blood cells. Phys Rev E 75:011921.

92. Wang N, Naruse K, Stamenovic D, Fredberg J, Mijailovich S, Tolic-Norrelykke I, Polte T, Mannix R, Ingber D (2001) Mechanical behavior in living cells consistent with the tensegrity model. Proc Natl Acad Sci 98:7765–7770.

93. Canadas P, Laurent V, Oddou C, Isabey D, Wendling S (2002) A cellular tensegrity model to analyse the structural viscoelasticity of the cytoskeleton. J Theor Biol 218:155–173.

94. Canadas P, Wendling-Mansuy S, Isabey D (2006) Frequency response of a viscoelastic tensegrity model: structural rearrangement contribution to cell dynamics. ASME J Biomech Eng 128:487–495.

95. Lu H, Schulten K (1999) Steered molecular dynamics simulations of force-induced protein domain unfolding. Proteins 35:453–463.

96. Lu H, Schulten K (2000) The key event in forceinduced unfolding of Titin's immunoglobulin domains. Biophys J 79:51–65.

97. Buehler MJ (2006) Atomistic and continuum modeling of mechanical properties of collagen: elasticity, fracture and self-assembly. J Mater Res 21:1947–1961.

98. Buehler MJ (2006) Nature designs tough collagen: explaining the nanostructure of collagen fibrils. Proc Natl Acad Sci 103:12285–12290.

99. Stultz C, Edelman E (2003) A structural model that explains the effects of hyperglycemia on collagenolysis. Biophys J 85:2198–2204.

100. Deshpande V, McMeeking R, Evans A (2006) A bio-chemical model for cell contractility. PNAS 103:14015–14020.

101. Herant M, Marganski W, Dembo M (2003) The mechanics of neutrophils: synthetic modeling of three experiments. Biophys J 84:3389–3413.

102. Vaziri A, Gopinath A, Deshpande V (2007) Continuum-based computational models in cell and nuclear mechanics. Journal of Mechanics of Materials and Structures 2(6):1169–1191.

103. Hu S, Chen J, Fabry B, Numaguchi Y, Gouldstone A, Ingber D, Fredberg J, Butler J, Wang N (2003) Intracellular stress tomography reveals stress focusing and structural anisotropy in cytoskeleton of living cells. Am J Physiol Cell Physiol 285:C1082–C1090.

104. Hu S, Chen J, Butler J, Wang N (2005) Prestress mediates force propagation into the nucleus. Biochem Biophys Res Commun 329:423–428.

105. Wang N, Suo Z (2005) Long-distance propagation of forces in a cell. Biochem Biophys Res Commun 328:1133–1138.

106. Blumenfeld R (2006) Isostaticity and controlled force transmission in the cytoskeleton: a model awaiting experimental evidence. Biophys J 91:1970–1983.

107. Chaturvedi R, Huang C, Kazmierczak B, Schneider T, Izaguirre A, Glimm T, Hentschel H, Glazier J, Newman S, Alber M (2005) On multiscale approaches to three dimensional modeling of morphogenesis. Journal of Royal Society Interface 2:237–253.

108. Dao M, Li J, Suresh S (2006) Molecularly based analysis of deformation of spectrin network and human erythrocyte. Mater Sci Eng C 26:1232–1244.

109. Gracheva M, Othmer H (2004) A continuum model of motility in ameboid cells. Bull Math Biol 66:167–193.

110. Liu A, Liu Y, Farrell D, Zhang L, Wang C, Fukui Y, Patankar N, Zhang Y, Bajaj C, Lee J, Hong J, Chen X, Hsu H (2006) Immersed finite element method and its applications to biological systems. Comput Methods Appl Mech Eng 195:1722–1749.

111. Ionides E, Fang K, Isseroff R, Oster G (2004) Stochastic models for cell motion and taxis. J Math Biol 48:23–37.

112. Rubinstein B, Jacobson K, Mogilner A (2005) Multiscale two-dimensional modeling of a motile simple-shaped cell. Multiscale Modeling & Simulation 3:413–439.

113. Maree A, Jilkine A, Dawes A, Grieneisen V, Edelstein-Keshet L (2006) Polarization and movement of keratocytes: a multiscale modelling approach. Bull Math Biol 68:1169–1211.

114. Zaman M, Trapini M, Sieminski A, MacKellar D, Gong H, Wells R, Lauffenburger D, Matsudaira P (2006) Migration of tumor cells in 3D matrices is governed by matrix stiffness along with cell-matrix adhesion and proteolysis. Proc Natl Acad Sci 103:10889–10894.

115. Xing J, Liao J-C, Oster G (2005) Making ATP. PNAS 102:15539–16546.

116. Liao J-C, Sun S, Chandler D, Oster G (2004) Conformational states of ATP:MG in water. Euro Biophys J 34:29.

117. Zaman M, Kaazempur-Mofrad M (2004) How flexible is α-actinin's rod domain? Mech Chem Biosys 1:291–302.

118. Yeung A, Evans E (1989) Cortical shell–liquid core model for passive flow of liquid-like spherical cells into micropipets. Biophys J 56:139–149.

119. Kan H, Shyy W, Udaykumar H, Vigneron P, Tran-Son-Tay R (1999) Effects of nucleus on leukocyte recovery. Ann Biomed Eng 27:648–655.

120. McElfresh M, Baesu E, Balhorn R, Belak J, Allen M, Rudd R (2002) Combining constitutive materials modeling with atomic force microscopy to understand the mechanical properties of living cells. Proc Natl Acad Sci 99:6493–6497.

121. Yang S, Saif M (2007) Force response and actin remodeling (agglomeration) in fibroblasts due to lateral indentation. Acta Biomaterialia 3:77–87.

122. Yang S, Saif MTA (2005) Micromachined force sensors for the study of cell mechanics. Rev Sci Instrum 76:044301.

123. Yang S, Saif T (2005) Reversible and repeatable linear local cell force response under large stretches. Exp Cell Res 305:42–50.

124. Serrel D, Oreskovic T, Slifka A, Mahajan R, Finch D (2007) A uniaxial bioMEMS device for quantitative force-displacement measurements. Biomedical Microdevices 9:267–275.

125. Zhu Y, Espinosa HD (2005) An electromechanical material testing system for in situ electron microscopy and applications. Proc Natl Acad Sci U S A 102:14503–14508.

126. Zhu Y, Moldovan N, Espinosa HD (2005) A microelectromechanical load sensor for in situ electron and X-ray microscopy tensile testing of nanostructures. Appl Phys Lett 86:013506.

127. Galbraith C, Sheetz M (1997) A micromachined device provides a new bend on fibroblast traction forces. PNAS 94:9114–9118.

128. Harris A, Wild P, Stopak D (1980) Silicone rubber substrata: a new wrinkle in the study of cell locomotion. Science 208:177–179.

129. Lin G, Pister K, Roos K (2000) Surface micromachined polysilicon heart cell force transducer. Journal of Microelectromechanical Systems 9:9–17.

130. Lin G, Wu V, Hainley R, Flanagan L, Monuki E, Tang W (2004) Development of a MEMS microsystem to study the effect of mechanical tension on cerebral cortex neurogenesis. In: Proceedings of the 26th annual international conference of the IEEE EMBS, San Francisco, CA.

131. Wu V, Law T, Hsu C-M, Lin G, Tang W, Monuki E (2005) MEMS platform for studying neurogenesis under controlled mechanical tension. In: Proceedings of the 3rd Annual International IEEE EMBS Special Topic, Kahuku, Oahu, Hawaii.

132. Koch S, Thayer G, Corwin A, de Boer M (2006) Micromachined piconewton force sensor for biophysics investigations. Appl Phys Lett 89:173901.

133. Eppell S, Smith B, Kahn H, Ballarini R (2005) Nano measurements with micro-devices: mechanical properties of hydrated collagen fibrils. Journal of the Royal Society Interface 3:117–121.

134. Scuor N, Gallina P, Panchawagh H, Mahajan R, Sbaizero O, Sergo V (2006) Design of a novel MEMS platform for the biaxial stimulation of living cells. Biomedical Microdevices 8:239–246.

135. Sun Y, Nelson B, Potasek D, Enikov E (2002) A bulk microfabricated multi-axis capacitive cellular force sensor using transverse comb drives. J Micromechanics Mircoengineering 12:832–840.

136. Li M, Tang H, Roukes M (2007) Ultra-sensitive NEMS-based cantilevers for sensing, scanned probe and very high-frequency applications. Nature Nanotechnology 2:114–120.

137. Bell DJ, Lu TJ, Fleck NA, Spearing SM (2005) MEMS actuators and sensors: observations on their performance and selection for purpose. J Micromechanics Microengineering 15:S153–S164.

138. Zhu Y, Corigliano A, Espinosa HD (2006) A thermal actuator for nanoscale in-situ microscopy testing: design and characterization. J Micromechanics Microengineering 16:242–253.

139. Conway N, Traina Z, Kim S-G (2007) A strain amplifying piezoelectric MEMS actuator. J Micromechanics Mircoengineering 17:781–787.

140. Indermuhle P-F, Schurmann G, Racine G-A, de Rooij N (1997) Atomic force microscopy using cantilevers with integrated tips and piezoelectric layers for actuation and detection. J Micromechanics Mircoengineering 7:218–220.

141. Park S-H, Lim E-C, Park K-S, Kang D-H, Han S-O, Lee D-C (1997) The dielectric properties of functional PVDF films by physical vapor deposition. In: Proceedings of the 5th International conference on properties and applications of dielectric materials, Seoul, Korea.

142. Atkinson G, Pearson R, Ouaies Z, Park C, Harrison J, Wilson W, Midkiff J (2003) Piezoelectric polyimide MEMS process. In: Proceedings of the NASA VLSI Symposium.

143. Bogart G, Carr D, Rogers J (2006) Fabrications of PVDF gratings: Final report for LDRD Project 79884. Sand Report SAND2005-6706. Sandia National Laboratories.

144. Jager EWH, Smela E, Inganas O (2000) Microfabricating conjugated polymer actuators. Science 290:1540–1545.

145. Smela E (2003) Conjugated polymer actuators for biomedical applications. Adv Mater 15:481–494.

146. Urdaneta M, Liu Y, Christophersen M, Prakash S, Abshire P, Smela E (2005) Integrating conjugated polymer microactuators with CMOS sensing circuitry for studying living cells. In: Smart structures and materials 2005: Electroactive Polymer Actuators and Devices (EAPAD).

147. Dargaville T, Celina M, Elliot J, Chaplya P, Jones G, Mowery D, Assink R, Clough R, Martin J (2005) Characterization, performance and optimization of PVDF as a piezoelectric film for advanced space mirror concepts. Sandia Report SAND2005-6846. Sandia National Laboratories.

148. Zu J, Qu Q, Cheng G (2004) Analytical modeling and quantitative analysis of scratch drive actuator. In: Proceedings of the 2004 International Conference on MEMS, NANO and Smart Systems (ICMENS'04).

149. de Boer M, Luck D, Ashurst W, Maboudian R, Corwin A, Walraven J, Redmond J (2004) High-performance surface-micromachined inchworm actuator. Journal of Microelectromechanical Systems 13:63–74.

150. Bronson J, Wiens G, Tran-Son-Tay R (2004) A feasibility study on MEMS test-structures for analysis of biological cells and tissue. In: Proceedings of 2004 Florida Conference on Recent Advances in Robotics, University of Central Florida in Orlando, Florida.

151. Liu W, Chen C (2005) Engineering biomaterials to control cell function. Materials Today 8:28–35.

152. Dusseiller M, Smith M, Vogel V, Textor M (2006) Microfabricated three-dimensional environments for single cell studies. Biointerphases 1:P1–P4.

153. Salaita K, Wang Y, Mirkin C (2007) Applications of dip-pen nanolithography. Nature Nanotechnology 2:145–155.

154. Lenhert S, Sun P, Wang Y, Fuchs H, Mirkin C (2007) Massively parallel dip-pen nanolithography of heterogeneous supported phospholipid mulitlayer patterns. Small 3:71–75.

155. Sameoto D, Hubbard T, Kujath M (2004) Operation of electrothermal and electrostatic MUMPs microactuators underwater. J Micromechanics Microengineering 2:250–255.

156. Sounart TL, Michalske TA, Zavadil KR (2005) Frequency-dependent electrostatic actuation in microfluidic MEMS. Journal of Microelectromechanical Systems 14:125–133.

157. Tinoco I, Li P, Bustamante C (2006) Determination of thermodynamics and kinetics of RNA reactions by force. Q Rev Biophys 39:325–360.

158. Hanley WD, Wirtz D, Konstantopoulos K (2004) Distinct kinetic and mechanical properties govern selectin-leukocyte interactions. J Cell Sci 117:2503–2511.

159. Miyazaki H, Hasegawa Y, Hayashi K (2000) A newly designed tensile tester for cells and its application to fibroblasts. J Biomech 33:97–104.

160. Sun S, Wirtz D (2006) Mechanics of enveloped virus entry into host cells. Biophysical Journal: Biophysical Letters 90:L10–L12.

161. del Monte F, O'Gara P, Poole-Wilson P, Yacoub M, Harding S (1995) Cell geometry and contractile abnormalities of myocytes from failing human left ventricle. Cardiovasc Res 30:281–290.

162. Campbell N, Mitchell L, Reece J (2002) Biology concepts and connections: Benjamin-Cummings, Redwood City, CA.

163. Pan W, Peterson E, Cai N, Ma G, Lee J, Feng Z, Liao K, Leong K (2005) Viscoelastic properties of human mesenchymal stem cells. In: Proceedings of the 2005 IEEE engineering in medicine and biology 27th annual conference, Shanghai, China.

164. Morii T, Mizumo R, Haruta H, Okada T (2004) An AFM study of the elasticity of DNA molecules. Thin Solid Films 464-465: 456–458.

165. Fauver M, Dunaway D, Lilienfeld D, Craighead H, Pollack G (1998) Microfabricated cantilevers for measurement of subcellular and molecular forces. IEEE Trans Biomed Eng 45:891–898.

166. Stamenovic D, Ingber D (2002) Models of cytoskeletal mechanics of adherent cells. Biomechanics and Modeling in Mechanobiology 1:95–108.

167. Ingber D (2003) Tensegrity II. How structural networks influence cellular information processing networks. J Cell Sci 15: 1397–1408.